Molecular Catalysis 484 (2020) 110741

Contents lists available at ScienceDirect

Molecular Catalysis

journal homepage: www.elsevier.com/locate/mcat

Molecular switch manipulating Prelog priority of an alcohol dehydrogenase toward bulky-bulky ketones

Xu Guochao, Dai Wei, Wang Yue, Zhang Lu, Sun Zewen, Zhou Jieyu, Ni Ye*

Key Laboratory of Industrial Biotechnology, Ministry of Education, School of Biotechnology, Jiangnan University, Wuxi 214122, Jiangsu, China

ARTICLE INFO

Keywords:
Alcohol dehydrogenase
Molecular switch
Prelog priority
Stereoselectivity
Bulky-bulky ketones
Substrate binding pocket

ABSTRACT

Structure-guided rational design revealed the molecular switch manipulating the Prelog and anti-Prelog priorities of an NADPH-dependent alcohol dehydrogenase toward prochiral ketones with bulky and similar substituents. Synergistic effects of unconserved residues at 214 and 237 in small and large substrate binding pockets were proven to be vital in governing the stereoselectivity. The *ee* values of E214Y/S237A and E214C/S237 G toward (4-chlorophenyl)-(pyridin-2-yl)-methanone were 99.3% (*R*) and 78.8% (*S*) respectively. Substrate specificity analysis revealed that similar patterns were also found with (4'-chlorophenyl)-phenylmethanone, (4'-bromophenyl)-phenylmethanone and (4'-nitrophenyl)-phenylmethanone. This study provides valuable evidence for understanding the molecular mechanism on enantioselective recognition of prochiral ketones by alcohol dehydrogenase.

1. Introduction

Optically active secondary alcohols are important building blocks in pharmaceutical, fine chemical, and food industries. Among them, enantiopure diaryl alcohols could serve as vital intermediates for antihistamine drugs such as (*S*)-betastine, (*R*)-neobenodine and (*S*)-carbinoxamine, and might also exhibit versatile pharmaceutical effects due to the great derivation potential of alcohol or aryl groups [1–3]. As a result, various approaches have been developed for the synthesis of chiral diaryl alcohols. Among them, asymmetric chemical reduction, transition metal-catalyzed hydrogenation, hydrogen transfer reduction of the corresponding diaryl ketones have provided useful accesses to chiral diaryl alcohols [4–6], however, with common drawback of limited substrate range and excess addition of transitional metals [7]. Enzymatic asymmetric reduction by carbonyl reductases or alcohol dehydrogenases offers necessary alternatives and has been applied in the synthesis of chiral alcohols [8].

Stereoselectivity is widely accepted as an intrinsic property of biocatalysts [9,10]. However, with regard to the reduction of diaryl ketones, such as (4-chlorophenyl)-(pyridin-2-yl)-methanone (CPMK, **1a**), few naturally-evolved reductases displayed high stereoselectivity [11–13]. For diaryl ketones with two similar aryl groups, *pro*-R and *pro*-S configurations could be generated in the enzymatic reduction since they are hard to be discriminated by the substrate binding pockets. Alcohol dehydrogenase from *Kluyveromyces polysporus*, designated as *Kp*ADH, could catalyze the asymmetric reduction of prochiral ketones with large substituents and follows Prelog's rule. However, bulky-bulky substrate **1a** was reduced by *Kp*ADH into (*R*)-(4-chlorophenyl)-(pyridin-2-yl)-methanone ((*R*)-CPMA, **1b**) with 82% *ee* according to the Cahn-Ingold-Prelog (CIP) priority (Scheme 1) [14], which was the same received by carbonyl reductase from *Sporobolomyces salmonicolor* (SSCR) [13]. Substrate **1a** and homologous diaryl ketones, are generally accepted as "difficult-to-reduce" ketones for carbonyl reductase [11]. SSCR had been evolved and a variant Q245 P was obtained, however, with moderate *ee* values (8–90%) toward diaryl ketones [13]. Commercial KRED124 and KRED60 have been reported to give (*R*) 94% *ee* and (*S*) 60% *ee* following Prelog and anti-Prelog's rule respectively [11]. *Km*CR2 was identified from *Kluyveromyces marxianus* CBS4857 by genome mining with the sequence of *Kp*ADH as a probe. *Km*CR2 displayed catalytic activity toward various diaryl ketones and also obeys Prelog priority in the asymmetric reduction of CPMK [15]. Most recently, *Tb*SADH from *Thermoanaerobacter brockii* and *Te*SADH from *Thermoanaerobacter pseudoethanolicus* were engineered to accept these bulky-bulky substrates [16,17]. However, these two ADHs belong to the zinc-dependent medium-chain dehydrogenases (MDR). It can be seen that the steric volume of 4-chlorophenyl and 2-pyridiyl substituents neighboring the carbonyl group of **1a** are quite similar, 111.2 and 104.8 Å^3 respectively. As expected, few naturally evolved carbonyl reductases displayed desirable capacity in stereoselective recognition of diaryl ketones. In addition, most of reductases obey Prelog's priority

* Corresponding author.
E-mail address: yni@jiangnan.edu.cn (Y. Ni).

https://doi.org/10.1016/j.mcat.2019.110741
Received 6 September 2019; Received in revised form 10 December 2019; Accepted 11 December 2019
Available online 19 December 2019
2468-8231/

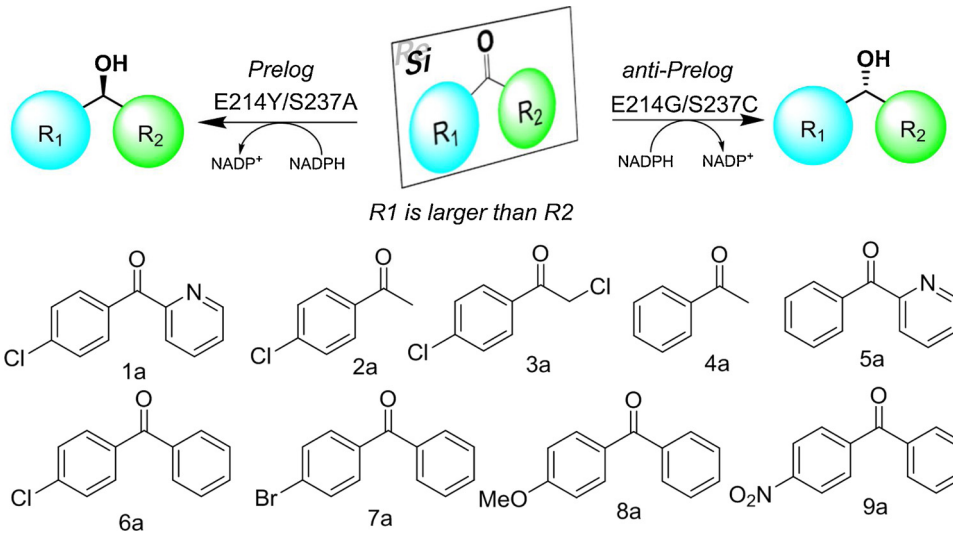

Scheme 1. Asymmetric reduction of bulky prochiral ketones (**1a–9a**) to the corresponding alcohols by (*R*)- and (*S*)-selective *Kp*ADH variants.

and produce (*R*)-**1b** [18,19]. Reductases with excellent anti-Prelog stereoselectivity are relatively rare [20,21], while some (*S*)-configured pharmaceuticals are more effective than corresponding (*R*)-enantiomer such as **1b** [22]. All above inspires us to identify residues modulating the stereoselectivity of *Kp*ADH and switching its stereoselectivity between Prelog's and anti-Prelog's priorities.

Several studies on the alteration of stereoselectivity toward ketones through site-directed mutagenesis have been reported due to lack of high throughput screening methods [23–25]. The results indicate that the stereoselectivity of reductases could depend on the relative sizes of two substituents besides carbonyl group. However, the nature of stereorecognition between enzyme and substrate and interactions for substrate orientation, especially toward diaryl ketones, remain elusive [26,27]. Identification of the molecular switch is of great fundamental and practical importance for the in-depth understanding of structure-function relationship of enzymes, enzyme-substrate interactions, and rational design of stereoselectivity.

2. Experimental

2.1. Reagents

Prochiral ketones, (4-chlorophenyl)-(pyridin-2-yl)-methanone (**1a**), (4-chlorophenyl)-methyl-methanone (**2a**), (4-chlorophenyl)-chloromethyl-methanone (**3a**), phenyl-methyl-methanone (**4a**), phenyl-(pyridin-2-yl)-methanone (**5a**), (4-chlorophenyl)-(phenyl)-methanone (**6a**), (4-bromophenyl)-(phenyl)-methanone (**7a**), (4-methoxyphenyl)-(phenyl)-methanone (**8a**) and (4-nitrophenyl)-(phenyl)-methanone (**9a**), were purchased from Aladdin (Shanghai) Co., Ltd.

2.2. Structural analysis and molecular dynamic simulations

Molecular dynamic simulations and structural analysis were performed as we previously reported employing crystal structure of *Kp*ADH in complex with $NADP^+$ (PDB accession No. 5Z2X) [25].

2.3. Site directed mutagenesis at E214 and S237

Saturation mutagenesis of E214 and S237 was performed by whole-plasmid PCR with pET28-*kpadh* as template and primers listed in Table S1. The PCR procedure was set as: predenaturation at 96 °C for 5 min, 20 cycles of denaturation at 98 °C for 15 s, annealing at 55 °C for 15 s and elongation at 68 °C for 3 min, further elongation at 68 °C for 10 min. The PCR products were verified by electrophoresis. Then, 5 μL PCR product was transferred to a new EP tube, followed by addition of 2.0 μL 10× buffer, 12.5 μL ddH_2O and 0.5 μL dpnI. The digestion mixture was maintained at 37 °C for 1 h to remove the template plasmids. Afterwards, 10 μL digestion mixture was transformed into *E. coli* BL21(DE3). Positive clones and mutagenesis were verified by colony PCR and sequencing.

Positive clones were picked up and inoculated into LB medium supplemented with kanamycin (50 μg mL^{-1}), and cultivated at 37 °C and 180 rpm. When the OD_{600} reached 0.6–0.8, 0.2 mM IPTG was added into the culture and further cultivated at 25 °C and 180 rpm for expression of recombinant enzymes. Then, the cells were collected by centrifugation at 8000 rpm and 4 °C. The cell pellets were resuspended with A buffer [20 mM PBS pH 7.4, 500 mM NaCl, 20 mM imidazole], disrupted by homogenizer (AH-BASICII, ATS Co., Ltd). Crude extract was obtained by centrifugation. Variants were purified by nickel affinity chromatography and eluted with gradient concentrations of imidazole. Purified variants were verified by SDS-PAGE. Variants were concentrated and further subjected to activity and stereoselectivity analysis.

2.4. Prelog selective and anti-Prelog selective combinatorial mutagenesis

Prelog selective combinatorial mutagenesis (Prelog library) was conducted by mixing plasmids of S237P, S237F, S237A, S237H, S237W and S237Y as templates and mixing primers of E214V, E214Y, E214I and E214F as primers. Since the concentrations of above-mentioned plasmids were different, plasmids were diluted according to the concentrations and kept at the same concentrations in the final mixture as shown in Table S2. Then whole plasmid PCR was performed as above described. Anti-Prelog selective combinatorial mutagenesis (anti-Prelog library) was also developed by mixing plasmids of E214R, E214S and E214G as templates and mixing primers of S237I and S237C and primers. The resultant PCR products were verified and digested with *dpn*I, and further transformed into *E. coli* BL21(DE3). For Prelog library, about 100 colonies were inoculated into 96-deep well plate and cultivated at 37 °C and 180 rpm. For anti-Prelog library, about 30 colonies were picked up and cultivated for induction of *Kp*ADH variants. All the variants were subjected to activity and stereoselectivity analysis.

2.5. Activity assay

The reductive and oxidative activities were spectrophotometrically determined by monitoring the absorbance changes of NADPH at 340 nm with molar extinction coefficient of 6220 $L{\cdot}mol^{-1}\,cm^{-1}$. The

reaction mixture was composed of 1 mM **1a**, 0.5 mM NADPH in PBS buffer (pH 6.0, 100 mM) and 10 μL enzyme solution with appropriated concentration at 30 °C. One unit of activity was defined as the amount of enzyme that catalyzed the oxidation of 1 μmol NADPH per minute under above mentioned condition.

2.6. Determination of kinetic parameters

Kinetic parameters of the purified *Kp*ADH variants was determined employing above mentioned activity assay method. The final substrate concentrations of **1a** were varied from 0.1 mM to 10 mM with 1.0 mM NADPH and appropriate of purified enzymes. All the activity was determined in triplicate. The K_m, V_{max} and k_{cat} were calculated according to the Lineweaver-Burk plot.

2.7. Analysis of substrate specificity

Substrate specificity of the purified *Kp*ADH variants toward **1a–9a** was analyzed by determination the specific activities using above described method. The final substrate concentrations of each substrate were 1.0 mM. All the activity was assayed in triplicate.

2.8. Bioconversion and determination of stereoselectivity

Six variants with significantly improved activity were selected to test their stereoselectivity and conversion rate. Bioconversion was conducted with 20 mM **1a–9a**, 20 U mL^{-1} *Kp*ADH or variants in PBS buffer (pH 7.0, 100 mM) in total volume of 2 mL at 30 °C and 180 rpm overnight. Then, 1 mL of the reaction mixture was withdrawn and extracted with equal volume of ethyl acetate. The organic phase was isolated by centrifugation at 12000 × *g* for 2 min, and dried over anhydrous $MgSO_4$. The conversion rate and stereoselectivity of the products were determined using the Agilent 1100 equipped with a Chiralcel OB-H column or a Chiralcel OD-H column (0.46 mm × 250 mm × 5 μm, Diacel, Japan). Detailed conditions for stereoselectivity analysis and the retention times of (*R*)- and (*S*)-alcohols could be found in Table S3 [28].

3. Results and discussion

3.1. Identification of key residues manipulating stereoselectivity of KpADH

Substrate **1a** was docked into the active center of *Kp*ADH. According to the diagram of the active center in Scheme 2, **1a** enters the substrate binding pocket (SBP) following an upside-down model with the carbonyl group orienting the bottom of the SBP, where locate the catalytic Tyr164 and cofactor NADPH. Residues S237 and E237 locate at the entrance of large and small SBP. The distance between S237 and 4-chlorophenyl group, and E214 and 2-pyridyl group, were calculated to be 3.4 and 3.5 Å, indicating there might exist direct interactions. Consensus analysis was also performed at correspondent positions of E214 and S237 among 100 homologous proteins with 40.6–54.7% sequence identities. Both sites were quite unconserved. At 214 equivalent position, there could be E, T, S, V, F, A, G, C, H and A, however, the neighboured positions were quite conversed with N and C at 213, S and T at 215. Similar pattern was found at 237 position, varied with S, G, A, N, C, T and F. Previously, conserved residues of carbonyl reductase *Dh*CR were found to play important roles in the catalytic efficiency toward α-chloroacetophenone, while almost no effect on stereoselectivity [29]. As a result, the unconserved residues, E214 and S237, were proposed to be crucial in manipulating the stereoselective recognition of substrates.

Saturation mutagenesis was performed at E214 and S237. All the variants were purified to homogeneity by nickel affinity chromatography (Fig. S1), and subjected to specific activity and stereoselectivity analysis (Fig. S2). None of the variants was deactivated hinting that position 214 has little influence on the catalytic activity. The specific activities of E214I, E214F, E214M and E214N were a little higher than that of wild type *Kp*ADH (WT). It is interesting to note that the stereoselectivity of WT was significantly influenced by mutation at E214. The highest and lowest *ee* values were 95.3% (*R*) of variant E214 V and 6.7% (*S*) of E214G. The stereopreference of WT was slightly reversed to anti-Prelog selective by single mutation, indicating the vital role of E214 in influencing the stereoselectivity. Moreover, in comparison with WT, variants E214Y, E214I and E214F also exhibited enhanced *ee* values (> 85%), whereas variants E214I, E214N, E214R, E214S and E214 G displayed decreased *ee* values (< 60%). In our previous study, S237 has been saturationally mutated [30], and the activity and stereoselectivity toward **1a** were illustrated in Fig. S2 with varied *ee* values ranging from 27.0% (*R*) to 96.1% (*R*). The *ee* values of variants S237A, S237P, S237F, S237W and S237Y were higher than 90% for (*R*), while those of S237I and S237C were lower than 50% for (*R*). It was presumed that positions 214 and 237 are the central residues of the small and large SBP respectively in manipulating the stereoselective recognition of substrates.

3.2. Combinatorial mutagenesis

Synergistic effect of E214 and S237 toward **1a** was explored by combinatorial mutagenesis among the variants with increased *ee* values (> 85%) as Prelog selective evolution (Prelog library) or decreased (< 60%) *ee* values for anti-Prelog selective evolution (anti-Prelog library). According to the CIP priority, for **1a**, variants with (*R*)-selectivity obey Prelog rule while variants with (*S*)-selectivity follow anti-Prelog rule. Most of the variants in Prelog library displayed *ee* values of over 85%, and about 20% of the variants exhibited > 96% *ee*, higher than the best variants in single mutation (E214 V and S237A) (Fig. 1A). The highest *ee* value was 99.3% (*R*) in Prelog library, followed by 98.8% (*R*), which were sequenced to be E214Y/S237A and E214 V/S237A respectively. With regard to the anti-Prelog library, the

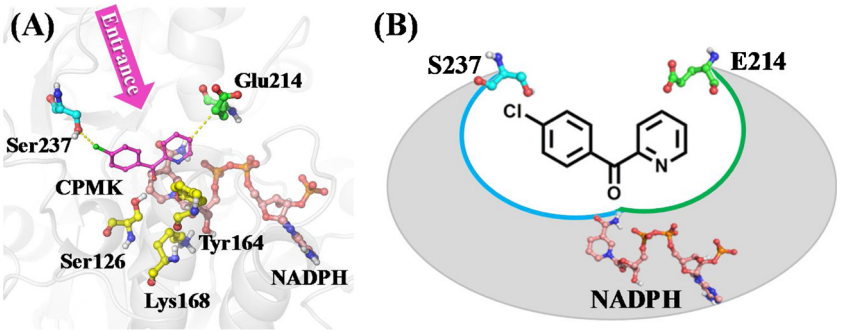

Scheme 2. Molecular docking of **1a** into *Kp*ADH (A) and illustration of S237 and E214 at the entrance of large and small substrate binding pockets (B). Catalytic triad Ser176-Tyr164-Lys168 was drawn in yellow, NADPH in pink, CPMK in violet, S237 in cyan, E214 in green.

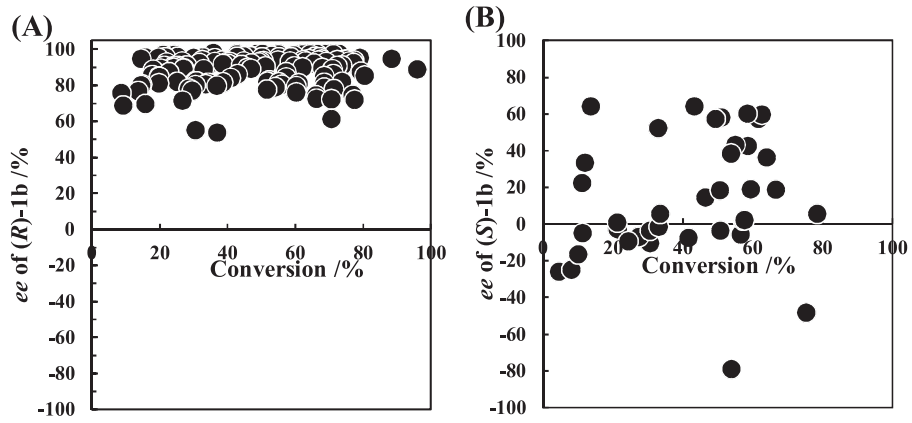

Fig. 1. Screening result of Prelog selective and anti-Prelog selective combinatorial mutagenesis libraries toward **1a**. (A) Prelog selective library, $ee = \frac{R-S}{R+S} \times 100\%$; (B) anti-Prelog selective library, $ee = \frac{S-R}{S+R} \times 100\%$. R and S denote the peak areas of (*R*)-**1b** and (*S*)-**1b**.

enantiopreference of about 40% variants was reverted to (*S*)-selective (Fig. 1B). It is noteworthy that the *ee* value of variant E214G/S237C was found to be 78.8% (*S*), much lower than the 82.4% (*R*) of WT, 27.0% (*R*) of S237C and 6.7% (*S*) of E214G. Considering the significantly increased *ee* of E214V/S237A and E214Y/S237A and the reverse stereopreference from (*R*) to (*S*) of E214G/S237C, a remarkable synergy effect in modulating stereoselectivity was found between E214 and S237 in SBP, since all the double variants were the combination of the best single mutants. It can be seen that 214Y/S237A and E214V/S237A follow Prelog priority and E214G/S237C obey anti-Prelog priority. According to the consensus analysis, at counterpart positions, there are T225/G237 in CgKR1, V222/C244 in Cg26 and T214/G237 in Gre2p (Fig. S3) [31–33]. In fact, CgKR1 and Cg26 obey Prelog priority in the reduction of prochiral ketones, while Gre2p follows anti-Prelog priority. Consequently, residues at 214 and 237 play vital role in manipulating the switch between Prelog and anti-Prelog priorities of short-chain dehydrogenase/reductases.

3.3. Kinetic parameters of KpADH and variants

Kinetic constants of single and double variants were determined (Table 1). Mutation of glutamate into valine and glycine resulted in decreased V_{max}, however, with increased binding affinity. Especially, E214G exhibited the lowest K_M of 0.25 mM among all the single and double variants. The V_{max} values of E214Y, S237A and S237C were slightly increased. For double variants, the K_M values of E214V/S237A and E214Y/S237A were 0.32 and 0.62 mM, much lower than 0.85 mM of WT, suggesting increased binding affinity toward **1a**. Although the k_{cat} of E214 V/S237A was decreased to 8.46 s^{-1}, the catalytic efficiency (k_{cat}/K_M) was increased to 26.6 s^{-1} mM^{-1} from 18.9 s^{-1} mM^{-1} of WT, mainly contributed to the significantly decreased K_M value by E214 V mutation. Both substrate binding affinity and activity of E214Y/S237A were increased, exhibiting k_{cat}/K_M of 25.5 s^{-1} mM^{-1}, 1.35-fold of WT. For the (*S*)-selective variant E214 G/S237C, the K_M and k_{cat} were 0.31 mM and 6.30 s^{-1}, resulting in k_{cat}/K_M of 22.1 s^{-1} mM^{-1}, higher than that of WT. Based on above analysis, there exists cooperative interaction between E214 and S237 not only in substrate binding but also in discriminating *pro*-R and *pro*-S conformations, and eventually working as a molecular switch in manipulating the stereoselectivity of *Kp*ADH.

Table 1
Kinetic parameters and *ee* values of WT and variants toward **1a**.

Variant	K_M [mM]	k_{cat} [s^{-1}]	k_{cat}/K_M [s^{-1}·mM^{-1}]	*ee*/Config. [%]
WT	0.85	16.1	18.9	82.4/(*R*)
E214V	0.43	8.91	21.2	95.3/(*R*)
E214G	0.25	5.50	22.1	6.7/(*S*)
E214Y	0.80	14.8	18.5	93.8/(*R*)
S237A	0.58	24.4	42.1	96.1/(*R*)
S237C	1.01	14.0	13.9	27.0/(*R*)
E214 V/S237A	0.32	8.46	26.6	98.9/(*R*)
E214Y/S237A	0.62	15.8	25.5	99.3/(*R*)
E214 G/S237C	0.31	6.30	22.1	78.8/(*S*)

3.4. Substrate profiles of KpADH, E214Y/S237A and E214 G/S237C

Substrate profiles of WT, (*R*)- and (*S*)-selective variants were characterized toward various prochiral ketones with large substituents (Scheme 1 and Table 2). The SBP of WT is so large that could accommodate all the ketones **1a–9a** tested. However, due to the relative bulky substituents at para position of aromatic ring, **7a–9a** were hard to be reduced by WT and variants. With regard to substrate 2a-4a with single bulky substituents, they were easily accepted by WT. The specific activity of WT toward **3a** was 44.0 U·mg^{-1} ranking the highest. However, the stereoselectivity of WT toward **2a**-**4a** was moderate, such as 86.9% toward **2a** and 95.2% toward **3a**. Moreover, WT also exhibited poor stereoselectivity toward bulky diaryl ketones, such as27.5% (*R*) of **5a**, 52.4% (*S*) of **6a**, 70.5% (*S*) of **7a**, 27.3% (*R*) of **8a** and 37.6% (*R*) of **9a** in *ee*. It can be seen that WT follows Prelog priority in the reduction of **1a**, **6a** and **7a**. However, with regard to **5a**, **8a** and **9a**, it is meaningless to define whether WT follows Prelog or anti-Prelog priority based on low *ee* values since it can not discriminate the two substituents.

The stereoselectivity of variant E214Y/S237A identified from Prelog selective library was greatly improved in comparison with WT, displaying (*R*) 99.3% *ee* toward **1a**, (*S*) 89.3% to **6a**, (*S*) 99.0% to **7a**, (*S*) 79.4% to **8a** and (*S*) 98.9% to **9a**. It should be noted that E214Y/S237A becomes strictly Prelog-selective and produces (*S*)-alcohols besides (*R*)-**1b** attributed to the CIP priority. The stereoselectivity of variant E214 G/S237C identified from anti-Prelog selective library was significantly altered, with *ee* values of (*S*) 78.8% toward **1a**, (*R*) 91.9% to **6a**, (*R*) 91.4% to **7a**, (*R*) 93.8% to **8a** and (*R*) 93.3% to **9a**, which are opposite to E214Y/S237A. Variant E214 G/S237C was also strictly anti-Prelog selective and produces (*R*)-alcohols besides (*S*)-**1b** due to the CIP priority. All the variants showed relatively higher *ee* toward **1a** than **5a**, proving the vital role of chloro group at para position of aromatic ring in the stereo-recognition. Similar pattern was also found in substrates **2a** and **4a**, elimination of the chloro group from substrates resulted in poor stereo-recognition. With regard to substrates **1a** and **6a** which are different in the 2'-pyridyl group, (*R*)-selective variants exhibited higher *ee* to **1a** than **6a**, while the (*S*)-selective variant preferred **6a–1a**, indicating different interactions between 2'-pyridyl group and E214V/Y or S237C. Moreover, unlike diaryl ketones, no apparent changes on stereopreference was found among variants toward the acetophenone derivatives (**2a–4a**), which might be attributed to the structural

Table 2
Specific activity and stereoselectivity of WT and variants toward various bulky ketones.

Substrate	WT		E214 V/S237A		E214Y/S237A		E214 G/S237C	
	Spec. act.[a] [U·mg $^{-1}$]	*e.e.*[%/(*R*/*S*)]	Spec. act. [U·mg $^{-1}$]	*e.e.*[%/(*R*/*S*)]	Spec. act. [U·mg $^{-1}$]	*e.e.*[%/(*R*/*S*)]	Spec. act. [U·mg $^{-1}$]	*e.e.*[%/(*R*/*S*)]
1a	18.4 ± 0.9	82.4 /*R*	12.0 ± 0.5	98.7 /*R*	22.0 ± 1.1	99.3 /*R*	9.65 ± 0.39	78.8 /*S*
2a	7.88 ± 0.32	86.9 /*R*	4.50 ± 0.09	97.8 /*R*	4.28 ± 0.13	97.9 /*R*	0.23 ± 0.01	97.4 /*R*
3a	44.0 ± 3.1	95.2 /*R*	57.7 ± 3.5	75.2 /*R*	54.7 ± 3.3	61.7 /*R*	20.9 ± 1.0	96.2 /*R*
4a	3.28 ± 0.13	37.0 /*R*	0.55 ± 0.02	17.2 /*R*	0.87 ± 0.02	32.1 /*R*	0.49 ± 0.01	99.1 /*R*
5a	11.8 ± 0.4	27.5 /*R*	8.30 ± 0.4	27.5 /*R*	11.8 ± 0.5	18.2 /*R*	9.00 ± 0.36	51.9 /*R*
6a	2.46 ± 0.07	52.4 /*S*	1.63 ± 0.05	−54.2 /*S*	0.99 ± 0.03	89.3 /*S*	1.82 ± 0.05	91.9 /*R*
7a	0.74 ± 0.03	70.5 /*S*	0.15 ± 0.01	−88.1 /*S*	0.36 ± 0.01	99.0 /*S*	0.15 ± 0.01	91.4 /*R*
8a	0.98 ± 0.03	27.3 /*R*	0.08 ± 0.02	−81.8 /*S*	0.77 ± 0.02	79.4 /*S*	0.08 ± 0.01	93.8 /*R*
9a	0.90 ± 0.03	37.6 /*R*	0.10 ± 0.01	−85.3 /*S*	0.12 ± 0.01	98.9 /*S*	0.10 ± 0.01	93.3 /*R*

Note: [a] Spec. act. denotes specific activity.

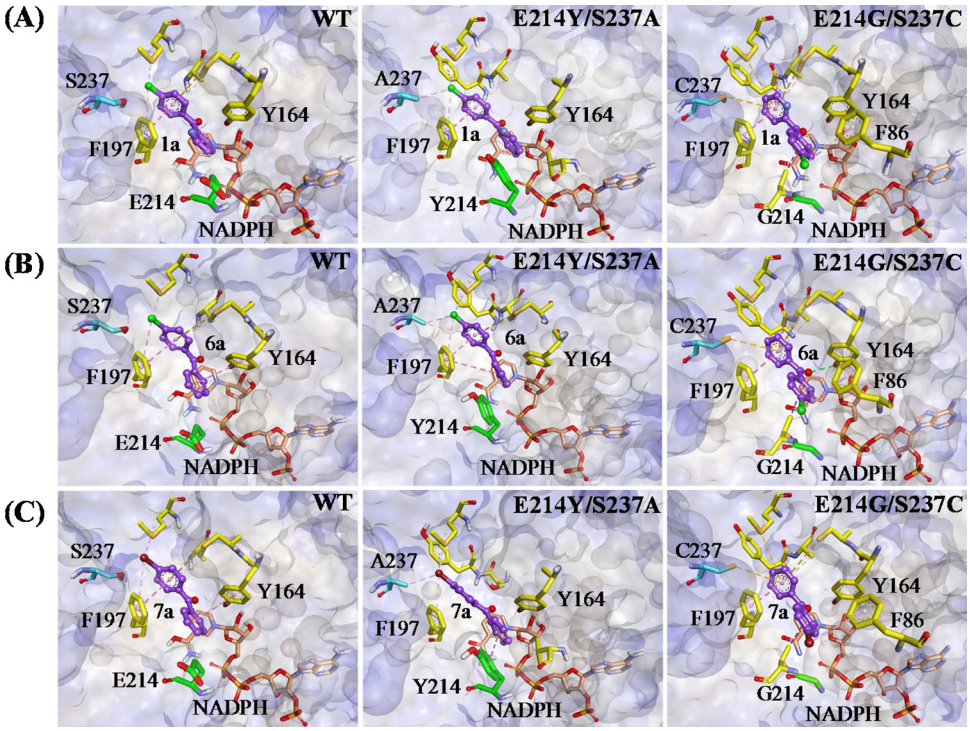

Fig. 2. Comparison of docking substrates **1a** (A), **6a** (B) and **7a** (C) in the active center of WT, E214Y/S237A and E214 G/S237C.

difference among them. In summary, the stereoselectivity of *Kp*ADH toward bulky-bulky substrates could be precisely manipulated by E214 and S237, converting between Prelog and anti-Prelog enzymes.

3.5. Interactions analysis of KpADH and variants towards bulky-bulky ketones

To understand the molecular basis of the altered stereopreference, molecular docking and dynamic simulations were performed (Fig. 2) (Fig. S4). In WT, only weak interactions (van der Waals) were found between chlorophenyl group and S237, and pyridyl group and E214, which is in consistent with the low stereoselectivity of WT. In E214Y/S237A, the larger tyrosine rendered a decreased small SBP, and the substrates would move toward the large SBP and closer to residue Ala237. Therefore, a new halo-alkyl bond could form between A237 residue and substrates (Fig. 2). The binding energy was decreased accordingly (Table S4). The conformations of **1a**, **6a** and **7a** in E214 G/S237C were completely inverted, resulting in the hydride transfer from *Re*-face to *Si*-face. Mutation of Ser at 237 into Cys led to decreased large SBP and increased polarity, which is unfavorable for the accommodation of chlorophenyl group. In cooperation with enlarged small SBP by introducing the smallest amino acid at 214, the chlorophenyl group rotated to the opposite direction. In addition, residue C237 could form extra sulfur-π interaction with pyridyl of **1a** and phenyl of **6a** and **7a**, contributing to stabilized *pro*-S state. More interactions could also accounted for the enhanced binding affinity between **1a** and E214G/S237C.

4. Conclusions

In summary, structure-guided rational mutagenesis was performed to identify the key residues as 'molecular switch' in manipulating the stereopreference of *Kp*ADH between Prelog and anti-Prelog priorities. The synergistic function of residues at 214 and 237 in E214Y/S237A and E214G/S237C was elucidated, including changes of substrate orientation, size of SBP and interactions between substrate and SBP. Significantly, the variants, E214Y/S237A and E214G/S237C, are more practical to stereoselectively accommodate prochiral ketones with large substituents neighboring carbonyl group. Our results suggest that the unconserved residues in SBP mainly modulate the substrate orientation and shapes of substrate binding pocket, and thus resulting in diverse stereoselectivity. This study could also provide guidance for

engineering the stereoselectivity of homologous carbonyl reductases toward similar substrates with special functional substituents.

CRediT authorship contribution statement

Methodology, Validation, Writing - original draft.Investigation, Visualization.Investigation, Visualization.Data curation.Data curation.Writing - review & editing.Supervision, Writing - review & editing.

Declaration of Competing Interest

None.

Acknowledgments

This work was financially supported by National Key R&D Program of China (2018YFA0901700), the National Natural Science Foundation of China (21776112), the national first-class discipline program of Light Industry Technology and Engineering (LITE2018-07), the Program of Introducing Talents of Discipline to Universities (111-2-06), and Top-notch Academic Programs Project of Jiangsu Higher Education Institutions for the financial support of this research.

Appendix A. Supplementary data

Supplementary material related to this article can be found, in the online version, at doi:https://doi.org/10.1016/j.mcat.2019.110741.

References

[1] F. Schmidt, R.T. Stemmler, J. Rudolph, C. Bolm, Catalytic asymmetric approaches towards enantiomerically enriched diarylmethanols and diarylmethylamines, Chem. Soc. Rev. 35 (2006) 454–470, https://doi.org/10.1039/b600091f.
[2] J.G. Kim, P.J. Walsh, From aryl bromides to enantioenriched benzylic alcohols in a single flask: catalytic asymmetric arylation of aldehydes, Angew. Chem. Int. Ed. 45 (2006) 4175–4178, https://doi.org/10.1002/anie.200600741.
[3] N.A. Magnus, P.B. Anzeveno, D.S. Coffey, D.A. Hay, M.E. Laurila, J.M. Schkeryantz, B.W. Shaw, M.A. Staszak, Optimized catalytic enantioselective aryl transfer process gives access to mGlu2 receptor potentiators, Org. Process Res. Dev. 11 (2007) 560–570, https://doi.org/10.1021/op0602268.
[4] C.Y. Chen, R.A. Reamer, J.R. Chilenski, C.J. McWilliam, Highly enantioselective hydrogenation of aromatic-heteroaromatic ketones, Org. Lett. 5 (2003) 5039–5042, https://doi.org/10.1021/ol0360795.
[5] K. Kriis, T. Kanger, M. Lopp, Asymmetric transfer hydrogenation of aromatic ketones by Rh(I)/bimorpholine complexes, Tetrahedron: Asymmetry 15 (2004) 2687–2691, https://doi.org/10.1016/j.tetasy.2004.07.017.
[6] Z. Dalicsek, F. Pollreisz, A. Goemoery, T. Soos, Recoverable fluorous CBS methodology for asymmetric reduction of ketones, Org. Lett. 7 (2005) 3243–3246, https://doi.org/10.1021/ol051024j.
[7] H.F. Duan, J.H. Xie, W.J. Shi, Q. Zhang, Q.L. Zhou, Enantioselective rhodium-catalyzed addition of arylboronic acids to aldehydes using chiral spiro monophosphite ligand, Org. Lett. 8 (2006) 1479–1481, https://doi.org/10.1021/ol060360c.
[8] U.T. Bornscheuer, G.W. Huisman, R.J. Kazlauskas, S. Lutz, J.C. Moore, K. Robins, Engineering the third wave of biocatalysis, Nature 485 (2012) 185–194, https://doi.org/10.1038/nature11117.
[9] E.L. Noey, N. Tibrewal, G. Iménez-Osés, S. Osuna, J. Park, C.M. Bond, D. Cascio, J. Liang, X. Zhang, G.W. Huisman, Y. Tang, K.N. Houk, Origins of stereoselectivity in evolved ketoreductases, Proc. Natl. Acad. Sci. U. S. A. 112 (2015) E7065–E7072, https://doi.org/10.1073/pnas.1507910112.
[10] Y.G. Zheng, H.H. Yin, D.F. Yu, X. Chen, X.L. Tang, X.J. Zhang, Y.P. Xue, Y.J. Wang, Z.Q. Liu, Recent advances in biotechnological applications of alcohol dehydrogenases, Appl. Microbiol. Biotechnol. 101 (2017) 987–1001, https://doi.org/10.1007/s00253-016-8083-6.
[11] M.D. Truppo, D. Pollard, P. Devine, Enzyme-catalyzed enantioselective diaryl ketone reductions, Org. Lett. 9 (2007) 335–338, https://doi.org/10.1021/ol0627909.
[12] I. Lavandera, A. Kern, B. Ferreira-Silva, A. Glieder, S. de Wildeman, W. Kroutil, Stereoselective bioreduction of bulky-bulky ketones by a novel ADH from *Ralstonia* sp, J. Org. Chem. 73 (2008) 6003–6005, https://doi.org/10.1021/jo800849d.
[13] H.M. Li, D.M. Zhu, L. Hua, E.R. Biehl, Enantioselective reduction of diaryl ketones catalyzed by a carbonyl reductase from *Sporobolomyces salmonicolor* and its mutant enzymes, Adv. Synth. Catal. 351 (2009) 583–588, https://doi.org/10.1002/adsc.200900045.
[14] J.Y. Zhou, G.C. Xu, R.Z. Han, J.J. Dong, W.G. Zhang, R.Z. Zhang, Y. Ni, Carbonyl group-dependent high-throughput screening and enzymatic characterization of diaromatic ketone reductase, Catal. Sci. Technol. 6 (2016) 6320–6327, https://doi.org/10.1039/c6cy00922k.
[15] Z.N. Li, Z.X. Wang, Y.H. Wang, X.F. Wu, H. Lu, Z.D. Huang, F.E. Chen, Substituent position-controlled stereoselectivity in enzymatic reduction of diaryl- and aryl (heteroaryl)methanones, Adv. Synth. Catal. 361 (2019) 1859–1865, https://doi.org/10.1002/adsc.201801543.
[16] M.M. Musa, O. Bsharat, I. Karume, C. Vieille, M. Takahashi, S.M. Hamdan, Expanding the substrate specificity of *Thermoanaerobacter pseudoethanolicus* secondary alcohol dehydrogenase by a dual site mutation, Eur. J. Org. Chem. 6 (2018) 798–805, https://doi.org/10.1002/ejoc.201701351.
[17] B.B. Liu, G. Qu, J.K. Li, W.C. Fan, J.A. Ma, Y. Xu, Y. Nie, Z.T. Sun, Conformational dynamics-guided loop engineering of an alcohol dehydrogenase: capture, turnover and enantioselective transformation of difficult-to-reduce ketones, Adv. Synth. Catal. 361 (2019) 3182–3190, https://doi.org/10.1002/adsc.201900249.
[18] P. Wang, J.B. Cai, Q. Ouyang, J.Y. He, H.Z. Su, Asymmetric biocatalytic reduction of 3,5-bis(trifluoromethyl) acetophenone to (1*R*)-[3,5-bis(trifluoromethyl)phenyl] ethanol using whole cells of newly isolated *Leifsonia xyli* HS0904, Appl. Microbiol. Biotechnol. 90 (2011) 1897–1904, https://doi.org/10.1007/s00253-011-3233-3.
[19] K. Goldberg, K. Schroer, S. Luetz, A. Liese, Biocatalytic ketone reduction – a powerful tool for the production of chiral alcohols – part II: whole-cell reductions, Appl. Microbiol. Biotechnol. 76 (2007) 249–255, https://doi.org/10.1016/10.1007/s00253-007-1005-x.
[20] P. Liang, B. Qin, M. Mu, X. Zhang, X. Jia, S. You, Prelog and anti-Prelog stereoselectivity of two ketoreductases from Candida glabrata, Biotechnol. Lett. 35 (2013) 1469–1473, https://doi.org/10.1007/s10529-013-1228-0.
[21] N. Itoh, Use of the anti-Prelog stereospecific alcohol dehydrogenase from *Leifsonia* and *Pseudomonas* for producing chiral alcohols, Appl. Microbiol. Biotechnol. 98 (2014) 3889–3904, https://doi.org/10.1007/s00253-014-5619-5.
[22] W.S. Jen, M.D. Truppo, D. Amos, P. Devine, M. McNevin, M. Biba, K. Campos, Copper-catalyzed synthesis of enantioenriched tetraarylethanes, Org. Lett. 10 (2008) 741–744, https://doi.org/10.1021/ol7027543.
[23] S.S. Wang, Y. Nie, Y. Xu, R.Z. Zhang, T.P. Ko, C.H. Huang, H.C. Chan, R.T. Guo, R. Xiao, Unconserved substrate-binding sites direct the stereoselectivity of medium-chain alcohol dehydrogenase, Chem. Commun. 50 (2014) 7770–7772, https://doi.org/10.1039/c4cc01752h.
[24] A.P. Li, L.D. Ye, X.H. Yang, C.C. Yang, J.L. Gu, H.W. Yu, Structure-guided stereoselectivity inversion of a short-chain dehydrogenase/reductase towards halogenated acetophenones, Chem. Commun. 52 (2016) 6284–6287, https://doi.org/10.1039/c6cc00051g.
[25] F.Y. Qin, B. Qin, W.H. Zhang, Y.L. Liu, X. Su, T.H. Zhu, J.P. Ouyang, J.Y. Guo, Y.X. Li, F.T. Zhang, X. Jia, S. You, Discovery of a switch between Prelog and anti-Prelog reduction toward halogen-substituted acetophenones in short-chain dehydrogenase/reductases, ACS Catal. 8 (2018) 6012–6020, https://doi.org/10.1021/acscatal.8b00807.
[26] M.M. Musa, M. Lott, M. Laivenieks, L. Watanabe, C. Vieille, R.S. Philips, A single point mutation reverses the enantiopreference of *Thermoanaerobacter ethanolicus* secondary alcohol dehydrogenase, ChemCatChem 1 (2009) 89–93, https://doi.org/10.1002/cctc.200900033.
[27] C.M. Nealon, M.M. Musa, J.M. Patel, R.S. Philips, Controlling substrate specificity and stereospecificity of alcohol dehydrogenases, ACS Catal. 5 (2015) 2100–2144, https://doi.org/10.1021/cs501457v.
[28] J.Y. Zhou, Y. Wang, G.C. Xu, L. Wu, R.Z. Han, U. Schwaneberg, Y.J. Rao, Y.L. Zhao, J.H. Zhou, Y. Ni, Structural insight into enantioselective inversion of an alcohol dehydrogenase reveals a "polar gate" in stereorecognition of diaryl ketones, J. Am. Chem. Soc. 140 (2018) 12645–12654, https://doi.org/10.1021/jacs.8b08640.
[29] G.C. Xu, Y.P. Shang, H.L. Yu, J.H. Xu, Identification of key residues in Debaryomyces hansenii carbonyl reductase for highly productive preparation of (*S*)-aryl halohydrins, Chem. Commun. 151 (2015) 15728–15731, https://doi.org/10.1039/c5cc06796k.
[30] Y. Wang, W. Dai, Y.M. Liu, Z.W. Zhang, J.Y. Zhou, G.C. Xu, Y. Ni, Fine tuning the enantioselectivity and substrate specificity of alcohol dehydrogenase from *Kluyveromyces polysporus* by single residue at 237, Catal. Commun. 108 (2018) 1–6, https://doi.org/10.1016/j.catcom.2018.01.012.
[31] H.M. Ma, L.L. Yang, Y. Ni, J. Zhang, C.X. Li, G.W. Zheng, H.Y. Yang, J.H. Xu, Stereospecific reduction of methyl *o*-chlorobenzoylformate at 300 $g{\cdot}L^{-1}$ without additional cofactor using a carbonyl reductase mined from *Candida glabrata*, Adv. Syn. Catal. 354 (2012) 1765–1772, https://doi.org/10.1002/adsc.201100366.
[32] I.A. Kaluzna, T. Matsuda, A.K. Sewell, J.D. Stewart, Systematic investigation of Saccharomyces cerevisiae enzymes catalysing carbonyl reductions, J. Am. Chem. Soc. 126 (2004) 12827–12832, https://doi.org/10.1021/ja0469479.
[33] G.C. Xu, Y.P. Zhang, Y. Wang, Y. Ni, Genome hunting of carbonyl reductases from Candida glabrata for efficient preparation of chiral secondary alcohols, Bioresour. Technol. 247 (2018) 553–560, https://doi.org/10.1016/j.biortech.2017.09.111.